OPEN ACCESS

Original research

Epigenetic promoter alterations in GI tumour immune-editing and resistance to immune checkpoint inhibition

Raghav Sundar,[1,2,3,4,5] Kie-Kyon Huang ,[3] Vikrant Kumar,[3] Kalpana Ramnarayanan,[3] Deniz Demircioglu,[6] Zhisheng Her,[7] Xuewen Ong,[3] Zul Fazreen Bin Adam Isa,[3,6,8] Manjie Xing,[3,6,8] Angie Lay-Keng Tan,[3] David Wai Meng Tai,[9] Su Pin Choo,[9,10] Weiwei Zhai,[6] Jia Qi Lim,[6] Meghna Das Thakur,[11] Luciana Molinero,[11] Edward Cha,[11] Marcella Fasso,[11] Monica Niger,[12] Filippo Pietrantonio,[12] Jeeyun Lee,[13] Anand D Jeyasekharan,[1,14] Aditi Qamra ,[15,16] Radhika Patnala,[17] Arne Fabritius,[17] Mark De Simone,[18] Joe Yeong,[7,14] Cedric Chuan Young Ng,[19] Sun Young Rha,[20,21] Yukiya Narita,[22] Kei Muro,[22] Yu Amanda Guo,[6] Anders Jacobsen Skanderup,[6] Jimmy Bok Yan So,[5,23,24] Wei Peng Yong,[1,5] Qingfeng Chen ,[7,25] Jonathan Göke,[6] Patrick Tan [3,5,6,14,26,27]

► Additional supplemental material is published online only. To view, please visit the journal online (http://dx.doi.org/10.1136/gutjnl-2021-324420).

For numbered affiliations see end of article.

Correspondence to
Dr Patrick Tan, Cancer and Stem Cell Biology Program, Duke-NUS Medical School, Singapore, Singapore; gmstanp@duke-nus.edu.sg and Dr Raghav Sundar, Department of Haematology-Oncology, National University Cancer Institute, Singapore; National University Hospital, Singapore, Singapore; raghav_sundar@nuhs.edu.sg

K-KH, VK, KR, DD and ZH contributed equally.

RS and PT are joint senior authors.

Received 15 February 2021
Accepted 3 August 2021

Check for updates

© Author(s) (or their employer(s)) 2021. Re-use permitted under CC BY-NC. No commercial re-use. See rights and permissions. Published by BMJ.

To cite: Sundar R, Huang K-K, Kumar V, *et al*. *Gut* Epub ahead of print: [*please include* Day Month Year]. doi:10.1136/gutjnl-2021-324420

ABSTRACT

Objectives Epigenomic alterations in cancer interact with the immune microenvironment to dictate tumour evolution and therapeutic response. We aimed to study the regulation of the tumour immune microenvironment through epigenetic alternate promoter use in gastric cancer and to expand our findings to other gastrointestinal tumours.

Design Alternate promoter burden (APB) was quantified using a novel bioinformatic algorithm (*proActiv*) to infer promoter activity from short-read RNA sequencing and samples categorised into APB_{high}, APB_{int} and APB_{low}. Single-cell RNA sequencing was performed to analyse the intratumour immune microenvironment. A humanised mouse cancer in vivo model was used to explore dynamic temporal interactions between tumour kinetics, alternate promoter usage and the human immune system. Multiple cohorts of gastrointestinal tumours treated with immunotherapy were assessed for correlation between APB and treatment outcomes.

Results APB_{high} gastric cancer tumours expressed decreased levels of T-cell cytolytic activity and exhibited signatures of immune depletion. Single-cell RNAsequencing analysis confirmed distinct immunological populations and lower T-cell proportions in APB_{high} tumours. Functional in vivo studies using 'humanised mice' harbouring an active human immune system revealed distinct temporal relationships between APB and tumour growth, with APB_{high} tumours having almost no human T-cell infiltration. Analysis of immunotherapy-treated patients with GI cancer confirmed resistance of APB_{high} tumours to immune checkpoint inhibition. APB_{high} gastric cancer exhibited significantly poorer progression-free survival compared with APB_{low} (median 55 days vs 121 days, HR 0.40, 95% CI 0.18 to 0.93, p=0.032).

Conclusion These findings demonstrate an association between alternate promoter use and the tumour microenvironment, leading to immune evasion and immunotherapy resistance.

Significance of this study

What is already known on this subject?

- Immune escape is a key factor for tumourigenesis.
- Epigenetic alterations in cancer interact with the immune microenvironment to control tumourigenesis and response to therapy.
- Studies in gastric cancer have shown an association between epigenetic alternate promoters, immune-editing and immune checkpoint inhibitor (ICI) resistance.

What are the new findings?

- Gastric tumours with higher epigenetic promoter alterations exhibited decreased levels of T-cell cytolytic markers and expressed signatures of immune depletion.
- These findings were orthogonally validated using novel technologies and platforms such as single-cell RNA sequencing and 'humanised mice'.
- Multiple gastrointestinal tumour types with higher alternate promoter burden also correlated significantly with poorer survival with ICI therapy.

How might it impact on clinical practice in the foreseeable future?

- Alternative promoter use burden may represent a negative predictive biomarker for immunotherapy applicable to multiple gastrointestinal tumour types.

INTRODUCTION

Tumour growth and metastases in the presence of robust host immunosurveillance is a hallmark of cancer. Immune-editing is a process harnessed by tumour cells to evade immune recognition using mechanisms such as modifications in antigen

Gut: first published as 10.1136/gutjnl-2021-324420 on 25 August 2021. Downloaded from http://gut.bmj.com/ on April 17, 2024 by guest. Protected by copyright.

presentation, dysregulation of immune checkpoints and immune-resistant clonal selection.[1–3] Previous studies have suggested that tumours may enhance immune-editing by co-opting epigenetic mechanisms such as DNA methylation, histone acetylation and chromatin modification to regulate T-cell reprogramming, neoantigen production and immune gene expression.[4–7] Notably, as epigenetic changes are potentially reversible, these represent potential nodes for anticancer therapeutic targets.[8]

We have previously described a novel mechanism of immune-editing in gastric cancer (or stomach adenocarcinoma (STAD)) using alternate promoters.[9 10] Promoters are *cis*-regulatory elements upstream of transcription start sites, and more than half of all human genes have multiple promoters.[11] Promoter activity is epigenetically regulated and use of alternate promoters can produce distinct 5′ untranslated regions and first exons, enhancing mRNA and protein isoform diversity.[12] Using epigenomic profiling, we demonstrated that a significant proportion of STADs can employ alternate promoters at highly expressed genes, generating 5′ truncated protein isoforms missing immunogenic N-terminal peptides. STADs with high levels of alternate promoter use were found to have an immunologically quiet phenotype and possible resistance to immune checkpoint inhibitor (ICI) therapy.[9 10]

In this study, we sought to study associations between alternate promoter use and the tumour immune microenvironment in gastric cancer, including temporal effects on tumour growth using a novel animal model. We expand our findings in gastric cancer to other gastrointestinal (GI) tumours by mining public datasets and using multiple immunotherapy-treated cohorts.

METHODS

Alternate promoter burden (APB) algorithm

APB was computed with a formula incorporating *proActiv*, an algorithm that estimates promoter activity from short-read RNA sequencing (RNA-Seq) data by mapping and quantifying first intron junctions of the genome. *proActiv* has been previously described and is available as an R package (online supplemental methods).[13] Samples were classified into groups: those in the top quartile of APB were classified as APB_{high}; those in the lowest quartile were classified as APB_{low}; and the rest of the samples were classified as APB_{int} (figure 1A). APB levels were normalised across batches/cohorts prior to categorising into groups.

Single-cell RNA-Seq of gastric cancer

Sample cohort description

Patients diagnosed with gastric adenocarcinoma and undergoing surgical resection at the National University Hospital, Singapore, were enrolled after obtaining written informed consent.

Single-cell RNA sequencing (scRNA-Seq) library preparation

Enriched 5′ gene expression libraries were constructed by generating gel beads in emulsion from single cells dissociated from tumour samples. Barcoded 10×, full-length cDNA was amplified via PCR, generating sufficient material to construct multiple libraries from the same cells. Libraries were subsequently sequenced on an Illumina Hiseq sequencer (online supplemental methods).

Single-cell gene expression quantification and determination of the major cell types

Unique molecular identified count matrices were first generated for each sample by passing the raw data in the cell ranger software. The count matrix was later used to generate a Seurat object which was used for clustering analysis.[14 15] Marker genes were compared for each cluster to literature-based markers of cell lineages to assign a cell lineage per cluster. Cell clusters were labelled based on curated and described cell markers.[16]

Humanised mouse model

All experiments and procedures were approved by the Institutional Animal Care and Use Committee (IACUC, IACUC# 191440) of A*STAR in accordance with guidelines of Agri-Food and Veterinary Authority and the National Advisory Committee for Laboratory Animal Research of Singapore.

Generation of humanised mice

One to three-day-old NOD-scid $Il2r\gamma^{null}$ (NSG) pups were sublethally irradiated at 1 Gy and engrafted with 1×10^5 human $CD34^+$ cord blood cells (HLA-A24:02, Stemcell Technologies) via intrahepatic injection. Mice with more than 10% human immune cell reconstitution (calculated based on the proportion of human CD45 relative to the sum of human and mouse CD45) were included in the study. In total, five cell lines of HLA-A24:02 subtype were selected for the experiment (two APB_{high} (SNU1750 and GSU), one APB_{int} (YCC21) and two APB_{low} (NCC 59 and SNU16) cell lines).

For each cell-line, five humanised mice and five NSG mice were injected with the tumour cells and observed for 1 month. Mice were sacrificed at the end of 1 month; necropsies was performed; and tumours were harvested for further analysis (online supplemental methods).

Immunotherapy-treated clinical cohorts

In a multicentre, industry-academic collaborative effort, a cohort of immunotherapy-treated GI cancer samples was collected to assess APB levels. A majority of the samples were from various ICI clinical trials conducted by the respective groups. The contributing site, tumour type, ICI treatment and type of transcriptomic analysis performed (RNA-Seq vs NanoString) are listed in online supplemental table S1. All patients were treated with ICIs in the metastatic, palliative intent setting.

Pan-cancer The Cancer Genome Atlas (TCGA) analysis

Gene expression data and clinical data from the PanCanAtlas were downloaded from Firebrowse.[17] Illumina HiSeq RNA-SeqV2 RSEM normalised gene values were used for correlations of *CD8A*, *GZMA* and *PRF1* and other immune correlates. All tumour types within the database were included except for tumours of haematological or immune origin (online supplemental methods).

Statistical analysis

Qualitative data in proportions were compared used Fisher's exact test. Two-sample t-test was used to compare parametric quantitative data. Wilcoxon rank-sum test was used to compare non-parametric quantitative data. Spearman's correlation was used for non-parametric bivariate quantitative comparisons. Kaplan-Meier curves and log-rank test were used for survival analysis. HRs and 95% CIs were evaluated using the Cox proportional hazards regression model. All analyses were done using R V.4.0.5.

RESULTS

RNA-Seq-based prediction of alternate promoter use enables pan-cancer analysis

H3K4me3 ChIP-Seq or Cap Analysis of Gene Expression tag sequencing are gold-standard techniques for detecting promoter activity.[18] However, data using these methods are typically

Gut: first published as 10.1136/gutjnl-2021-324420 on 25 August 2021. Downloaded from http://gut.bmj.com/ on April 17, 2024 by guest. Protected by copyright.

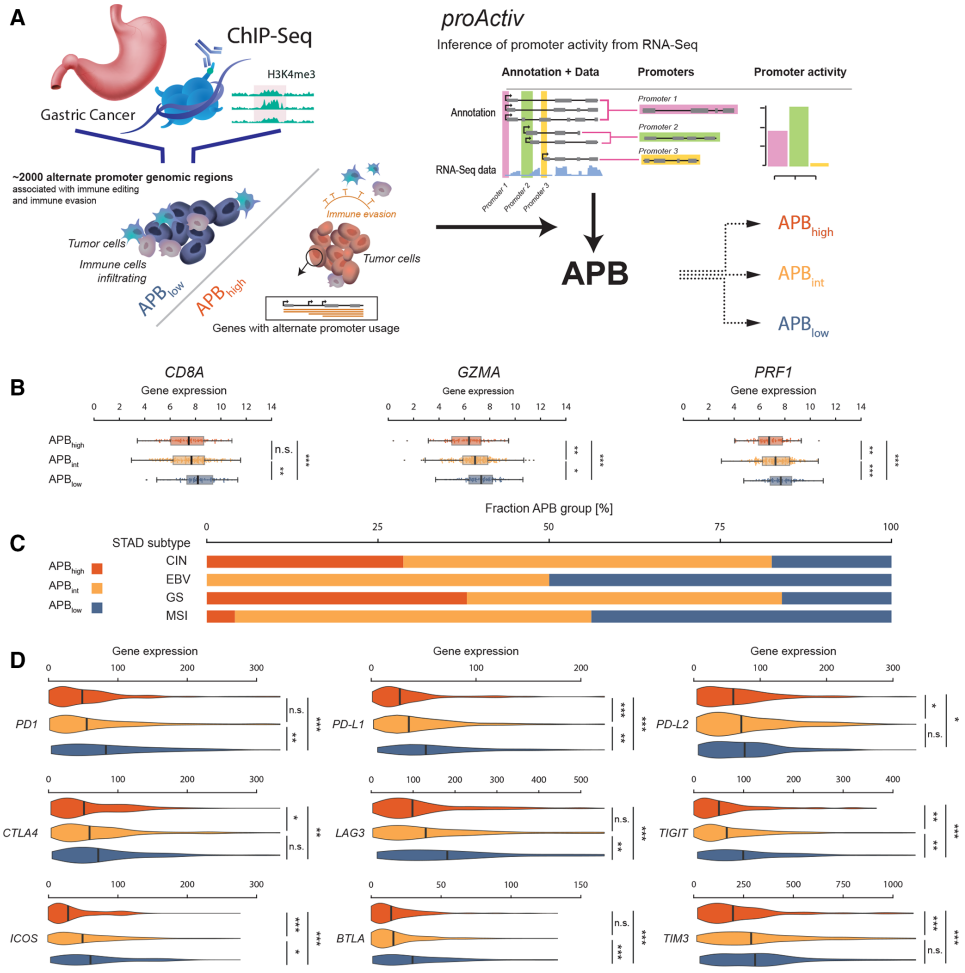

Figure 1 Development of RNA-Seq-based algorithm to measure alternate promoter use. (A) Epigenetic chromatin immunoprecipitation sequencing (ChIPSeq) study in gastric cancer identified specific gain-of-expression ('gain promoters') and loss-of-expression ('loss promoters') genomic regions which were associated with immune-editing in gastric cancer. In total, approximately 2000 alternate promoter genomic regions were identified. *proActiv* algorithm is employed to infer promoter activity from short-read bulk RNA-Seq data. *proActiv* infers promoter activity by quantifying first intron junctions of RNA-Seq transcripts. Genomic regions identified from ChIPSeq data are combined with *proActiv* to quantify APB. Samples within each cohort were classified into groups based on APB: APB_{high}, APB_{int} and APB_{low}. (B) Association of APB groups in STAD with established markers of T-cell cytolytic activity (*CD8A*, *GZMA* and *PRF1*). APB_{high} group is denoted in red, APB_{int} in yellow and APB_{low} in blue. APB_{high} group shows lower expression of these three genes compared with APB_{int}, which in turn shows a lower expression to the APB_{low} group (Wilcoxon test; ***p<0.001, **p<0.01, *p<0.05; n.s.). (C) Distribution of STAD TCGA subtypes by the APB group. STAD TCGA molecular subtypes: CIN, GS, EBV associated and MSI. (D) Association of APB groups in STAD with nine selected immune checkpoints. Similar to markers of T-cell activity, expression of these nine checkpoints is consistently lower in APB_{high} (red) compared with APB_{int} (yellow) and APB_{low} (blue). (Wilcoxon test; ***p<0.001, **p<0.01, *p<0.05; n.s.). APB, alternate promoter burden; CIN, chromosomal unstable; EBV, Epstein-Barr virus associated; GS, genome stable; MSI, microsatellite instability; n.s., not significant; STAD; stomach adenocarcinoma; TCGA, The Cancer Genome Atlas.

available only for small tumour cohorts, and not for large datasets or clinical trial populations. To overcome these limitations, we harnessed *proActiv*, a previously described bioinformatic algorithm to infer promoter activity from short-read RNA-Seq data.[13 19] We employed *proActiv* to estimate tumour-associated promoter changes using a predefined set of alternate promoters corresponding to epigenomic regions gained or lost in primary STADs relative to matched normal gastric tissues, determined by previous H3K4me3 ChIP-seq.[9] Dysregulated alternate promoters identified by *proActiv* were quantified, generating for each tumour a sample-specific 'APB' score (APB) (figure 1A).

First, we computed APB for 416 STAD samples from TCGA. The STAD samples were categorised as APB_{high}: n=103 (25%), APB_{int}: n=210 (50%) and APB_{low}: n=103 (25%). APB_{high} tumours exhibited decreased expression of the T-cell cytolytic markers *CD8A* (CD8 + tumour-infiltrating lymphocytes (TILs)), *GZMA* (granzyme A) and *PRF1* (perforin 1) (APB_{high} vs APB_{low}, Wilcoxon test, p<0.001; figure 1B).[20] As a negative control, correlations to *CD8A*, *GZMA* and *PRF1* expression were not observed when APB was calculated using randomly selected promoter subsets of similar size (empirical p<0.01). These results are similar to previous observations in STAD, supporting the use of *proActiv* to infer promoter activity from RNA-Seq data.[9 13]

To investigate relationships between APB and the four TCGA STAD molecular subtypes: chromosomal unstable (CIN), genome stable (GS), Epstein-Barr virus associated (EBV) and microsatellite instability (MSI), we analysed 376 STADs where TCGA subtype classification was available. MSI and EBV subtypes were found to have few/no APB_{high} tumours (4% and 0%, respectively), while CIN and GS subtypes had significantly higher proportions of APB_{high} tumours compared with APB_{low} tumours (29% vs 17%, p<0.0001, and 38% vs 16%, p=0.012,

Gut: first published as 10.1136/gutjnl-2021-324420 on 25 August 2021. Downloaded from http://gut.bmj.com/ on April 17, 2024 by guest. Protected by copyright.

respectively) (figure 1C). There were no significant differences between APB groups when categorised by Lauren's histological subtype (ie, diffuse vs intestinal) (online supplemental figure S1A). The APB groups were also correlated with nine immune checkpoint genes of therapeutic relevance (*PD-1*, *PD-L1*, *PD-L2*, *CTLA4*, *LAG3*, *TIM3*, *ICOS*, *BTLA* and *TIGIT*). All immune checkpoint genes displayed lower expression in APB_{high} tumours compared with APB_{low} ($p \leq 0.01$ for all nine genes) (figure 1D). After excluding MSI tumours, there was no difference in tumour mutation burden (TMB) between APB_{low} and APB_{high} tumours (3.6 vs 3.0 muts/Mb, p=0.12) (online supplemental figure S1B).

To study the effect of tumour–stroma composition, we correlated APB with tumour purity obtained from a consensus estimation method.[21] We found only a weak positive correlation between tumour content and APB (Pearson r=0.09, p=0.062) (online supplemental figure S1C). These findings suggest that the estimation of alternate promoter use by the tumours is not merely driven by the fraction of cancer cells within a tumour sample. Next, we correlated the relative proportions of major immune cell types (from CIBERSORT) of the TCGA STAD samples.[22] Consistent with previous analysis, APB_{low} tumours had higher T-cell abundance (CD4 (p=0.0068), CD8 (p=0.011) and T follicular helper cells (p=0.033)), and macrophage M1 abundance (p=0.039). In contrast, APB_{high} had higher abundance of mast cells (p=0.0079) (online supplemental figure S1D–H), suggesting a possible role of innate immunity in APB_{high} tumours. We also correlated APB with intratumour heterogeneity scores calculated by ABSOLUTE.[22] APB_{high} tumours appeared to have higher intratumour heterogeneity than the APB_{low} tumours (p=0.022) (online supplemental figure S1I).

scRNA-Seq confirms distinct immunological populations in APB_{high} and APB_{low} tumours

To further investigate if APB_{high} tumours have distinct or reduced tumorous immune-cell infiltrates compared with APB_{low} tumours, we performed scRNA-Seq.We generated paired bulk RNA-Seq and scRNA-Seq data (55 071 cells) on 11 surgically resected primary STAD samples (APB can be derived only from bulk RNA-Seq as measurements of RNA at isoform-specific levels are below the limits of detection of current scRNA-Seq technology), classifying 3 samples as APB_{low} (19 920 cells), 5 as APB_{int} (18 335 cells) and 3 as APB_{high} (16 816 cells) (online supplemental table S2). To identify cellular populations, unsupervised cell clustering based on gene expression profiles was performed, allowing for dimensionality reduction to six major cell types: T cells, epithelial cells, B cells, macrophages, endothelial cells and fibroblasts (figure 2A).

Expressions of *CD8A*, *GZMA*, *PRF1* and immune checkpoint genes were studied within the specific cellular populations. *CD8A*, *GZMA* and *PRF1* were expressed almost exclusively within T cells (~40% to 55% of T cells) validating the expression of *CD8A*, *GZMA* and *PRF1* in bulk RNA-Seq as appropriate surrogates for T-cell cytolytic activity (online supplemental figure 2A). Similarly, immune checkpoints traditionally described as expressed on T cells such as *PD-1*, *LAG3*, *TIGIT*, *TIM3*, *CTLA4* and *ICOS* had significantly higher single-cell transcript expression in T cells (online supplemental figure S2A). We compared cellular proportions between the APB groups (online supplemental figure S2B). Overall, T-cell proportions were higher in APB_{low} tumours compared with APB_{int}/APB_{high} tumours (42% vs 30%, p<0.0001) (figure 2B). In contrast, epithelial cell proportions were lower in APB_{low} tumours (13% vs 21%, p<0.0001). Notably, there were no significant differences in B-cell composition between the groups (14% vs 14%, p=0.82) (online supplemental table S3). APB_{low} tumours had significantly higher expression of *CD8A*, *GZMA* and *PRF1* within T cells compared with APB_{high} tumours (Wilcoxon p<0.0001), supporting the bulk RNA-Seq analysis. Immune checkpoints also had significantly higher expression in APB_{low} tumours compared with APB_{high} tumours (Wilcoxon p<0.0001) (figure 2C and online supplemental figure S2C), similar to bulk RNA-Seq data. Taken collectively, these results highlight distinct tumour immune microenvironments and regulation of immune checkpoints between tumours with high and low alternate promoter uses.

Interaction between alternate promoter use and the immune system in a humanised-mouse model

Analysis of primary tumours often represents only a single temporal snapshot of the tumour, obtained at the time of surgical resection or biopsy. To explore dynamic temporal interactions between tumour kinetics, alternate promoter usage and the human immune system, we used a humanised-mouse cancer in vivo model. NOD-scid $Il2r\gamma^{null}$ (NSG) immune-deficient mice pups were engrafted with HLA-A24:02 human umbilical cord blood $CD34^+$ cells, and mice with postengraftment human immune-cell reconstitution (termed 'humanised mice') were selected for the study. Five HLA-A24:02 subtype STAD cell lines (two APB_{high}, one APB_{int} and two APB_{low} cell lines) were selected (online supplemental table S4). These cell lines were either commercially available or acquired from academic collaborators.[23–25] For each STAD cell line, five humanised mice and five NSG immune-deficient mice were injected subcutaneously in the flank with tumour cells. The resulting tumours were analysed for growth rate, tumour size, mass, volume and histopathological analysis (figure 3A).

Reflecting the importance of studying tumour growth kinetics within the context of an active immune system, tumour uptake and growth initiation were faster in NSG compared with humanised mice: 97% of NSG and 63% of humanised mice developed a tumour by day 7 (Fisher's exact p=0.00056). Notably, APB_{high} and APB_{int} cell lines exhibited faster tumour growth rates compared with APB_{low} cell lines in humanised mice, consistent with APB_{high} tumours exhibiting immune escape potential and demonstrating tumourigenesis in an active immune system. Specifically, in the humanised mice, APB_{high} cell lines had 90% tumour development (vs 100% in immune-deficient mice); APB_{int} had 100% tumour development (vs 100% in immune-deficient); and APB_{low} had 20% (vs 93% in NSG) tumour development by day 7 (APB_{high}/APB_{int} vs APB_{low}, Fisher's exact p=0.039). Growth rates between NSG and humanised mice were compared for each cell line. For APB_{high} and APB_{int} cell lines, tumours in humanised mice appeared to grow faster than tumours in NSG mice, while the converse was observed for APB_{low} cell lines, with tumours in NSG mice growing faster than humanised mice (figure 3B). By the end of the experiment, APB_{low} tumours grown in humanised mice were smaller than those grown in NSG mice (median 375 mm^3 vs 512 mm^3, p=0.033). In contrast, for APB_{int} and APB_{high} cell lines, humanised-mice tumours trended towards being larger than those grown in NSG mice (median 418 mm^3 vs 257 mm^3, p=0.073).

At the end of 1 month, mice were sacrificed, and tumours were harvested and analysed by microscopy and immunohistochemistry. APB_{low} tumours showed significant human T-cell infiltration into tumours, while APB_{high} tumours had almost no human T-cell infiltration (figure 3C). APB_{low} tumours had significantly higher CD3+ (broad T-cell marker) cellular infiltration compared with

Gut: first published as 10.1136/gutjnl-2021-324420 on 25 August 2021. Downloaded from http://gut.bmj.com/ on April 17, 2024 by guest. Protected by copyright.

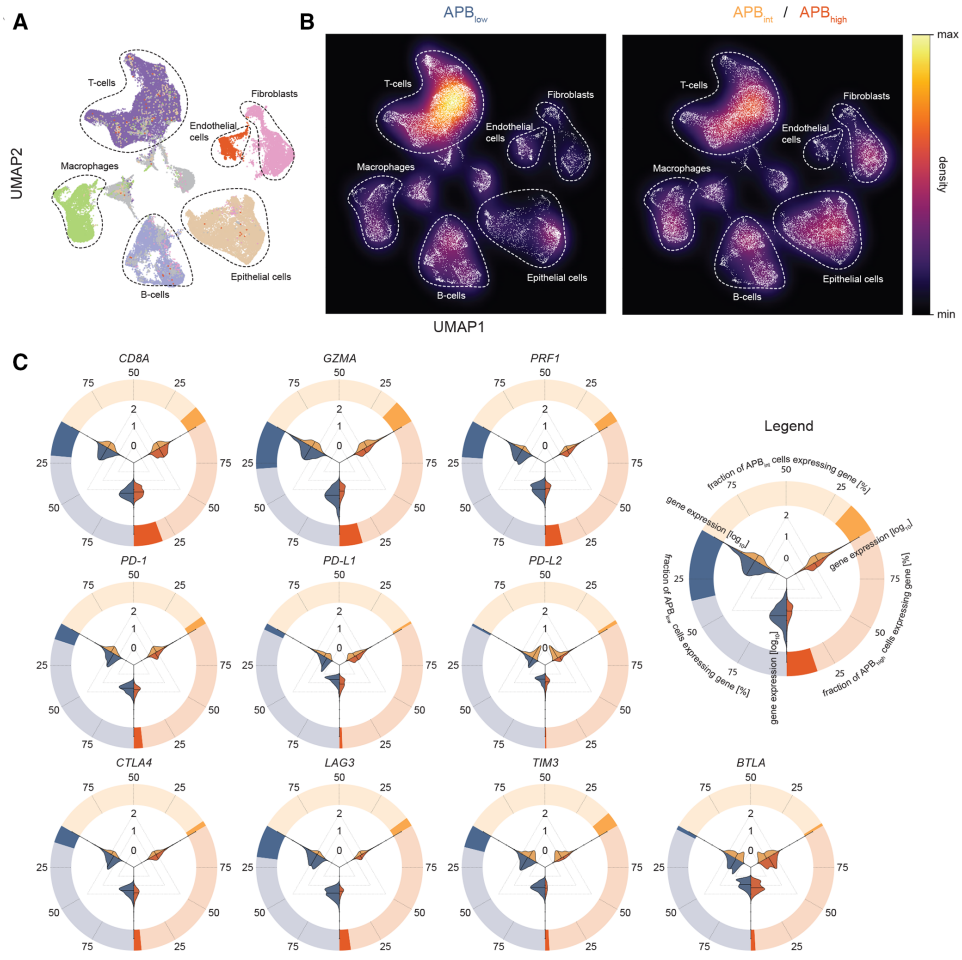

Figure 2 Single-cell RNA-Seq of gastric cancer and association with APB with the tumour microenvironment. (A) UMap of 55 071 gastric cancer cells from 11 samples (3 APB_{high}, 5 APB_{int}, 3 APB_{low}) to visualise cell types and clusters. Unsupervised hierarchical clustering was performed to generate clusters, which were then mapped and labelled based on expression of known marker genes. Major cell types include epithelial cells (brown), T cells (deep purple), B cells (light purple), endothelial cells (red), fibroblasts (pink) and macrophages (green). (B) Density plot of UMap in (A) stratified by APB_{low} versus APB_{int}/APB_{high} highlighting the higher proportion of T cells in the APB_{low} tumours and epithelial cells in APB_{int}/APB_{high} tumours. (C) Circle–violin plots of expression of *CD8A*, *GZMA* and *PRF1* and immune checkpoints by the APB group in scRNA-Seq. The outer circle demonstrates the proportion of cells within the APB group which express the gene. For example, ~25% of cells in APB_{low} tumours (blue) express *CD8A*, while less than 25% of cells in APB_{high} (red) and APB_{int} (yellow) tumours express this gene. The violin plots within depict the magnitude of expression by the APB group. Three comparisons are made: APB_{low}(blue) versus ABP_{int} (yellow); APB_{int} versus APB_{high}(red) and APB_{low} versus APB_{high}. From the violin plots, it is evident that the cells that do express the genes within each APB group are similar, yet, much fewer of these cells exist in APB_{int} and APB_{high} tumours compared with APB_{low}. These results suggest that while *CD8A*-positive cells are present in APB_{high} and APB_{int} tumours, much lower levels of *GZMA* and *PRF1* are expressed by these cells. APB, alternate promoter use burden; scRNA-Seq, single-cell RNA sequencing.

APB_{high} tumours (15% vs 4%, p=0.0085), and a trend towards higher CD8+ (cytotoxic T-cell marker) cellular infiltration (10% vs 2%, p=0.088) (figure 3D). Next, we performed bulk RNA-Seq on the tumours harvested from the humanised mice at the end of the experiment, studying the expression of genes marking specific cellular subtypes. APB_{low} tumours exhibited higher levels of both adaptive immunity cells (*CD8A* and *PRF1* (cytotoxic T cells)) and innate immunity cells (*PLD4* (dendritic cells) and *CD163* (macrophages)) (online supplemental figure S3A). In contrast, APB_{high} tumours grown in humanised mice did not show these features and demonstrated higher levels of only dendritic cells and macrophages (*PLD4* and *CD163*, associated with innate immunity) (online supplemental figure S3B). In addition to immune cell types, we also studied expression of immune checkpoints in the tumours grown in humanised mice. APB_{low} tumours expressed higher levels of *LAG3*, a marker of T-cell exhaustion, and *TIM3* (online supplemental figure S3C,D). These findings from the humanised-mouse model indicate that APB_{high} tumours are likely to have the ability to evade the immune system and have an immunologically quiet phenotype, supporting orthogonal findings in primary tumours at both the bulk and single-cell levels.

High alternate promoter use is associated with resistance to ICIs across multiple tumour types

Early evidence has suggested that APB_{high} STADs may be resistant to ICI therapy.[10] We sought to build on those findings and to validate the hypothesis that APB_{high} tumours are resistant to ICIs due to their immunologically quiet phenotype. APB was calculated from RNA-Seq data of 53 gastric cancer samples treated with pembrolizumab, nivolumab or atezolizumab (monoclonal antibodies against PD-1/PD-L1). The median age was 57 years and 75% were male (online supplemental table S5). All patients

Gut: first published as 10.1136/gutjnl-2021-324420 on 25 August 2021. Downloaded from http://gut.bmj.com/ on April 17, 2024 by guest. Protected by copyright.

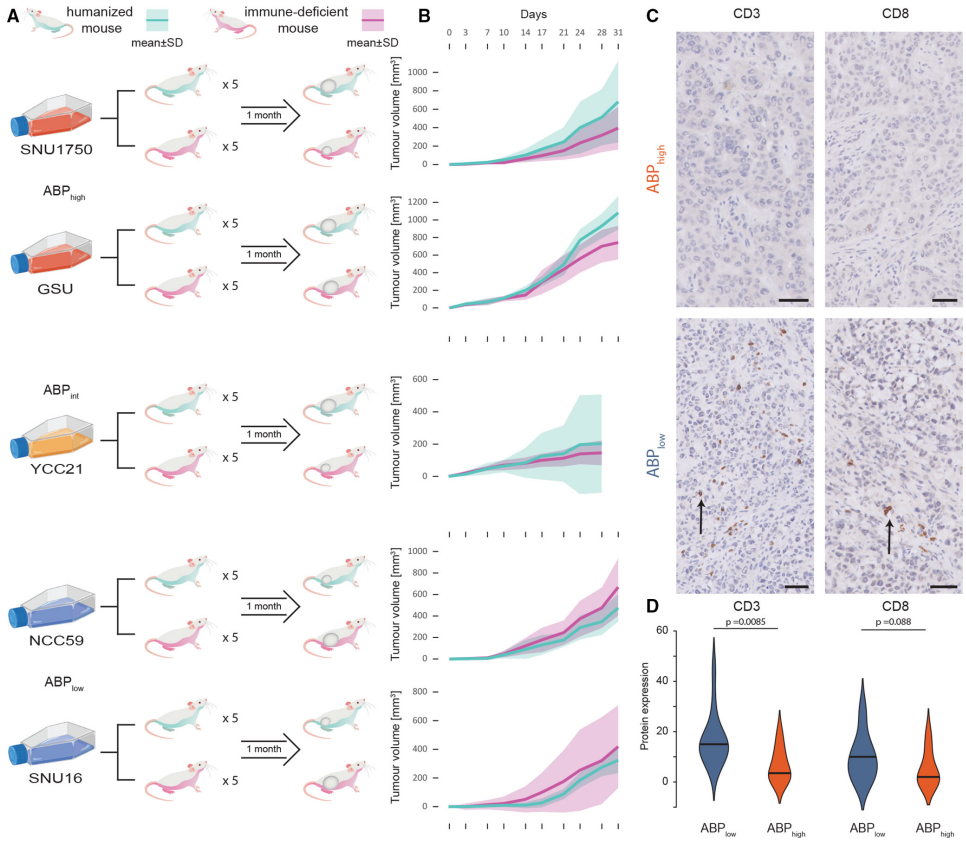

Figure 3 Humanised-mice model study of APB. (A) Study schema of humanised-mouse model experiment. Five cell lines were used (two APB_{high}, one APB_{int} and two APB_{low} cell lines each). For each cell line, five humanised mice and five immune-deficient NSG mice were injected subcutaneously in the flank with the tumour cells and observed for 1 month. Mice were sacrificed at the end of 1 month, necropsies performed and tumours harvested for analysis. (B) Tumour growth in humanised mice versus NSG mice by APB group. Cyan lines are humanised mice; magenta lines are NSG mice. APB_{high} and APB_{int} tumours have faster growth in humanised mice compared with NSG mice, while in APB_{low} tumours, humanised mice have slower growth compared with NSG mice. (C) Histology of tumours harvested from humanised mice with tumour growth. CD3 and CD8 immunohistochemistry staining imaging shows heavy TILs in SNU16 (APB_{low}) (black arrows) and no infiltration in SNU1750 (APB_{high}). APB_{high} tumours had significantly lower levels of CD3 + and CD8+ T-cell infiltration into the tumour. Black bar magnification 50 µm. (D) Expression of CD3 and CD8 by immunohistochemistry scoring in humanised-mouse tumours by the APB group. Immunohistochemical and H&E staining was performed on the FFPE tissue with antibodies targeting CD3 and CD8. The percentage of cells displaying unequivocal staining of any intensity for CD3 or CD8 were determined by a pathologist blinded to clinicopathological and survival information. TILs expressing CD3 or CD8 were identified within the intratumoral area defined as lymphocytes within cancer cell nests and in direct contact with tumour cells. Quantification of TILs was determined by the percentage of the intratumoral areas occupied by the respective TIL population. Violin plots highlight the expression of CD3 and CD8 within these cells by the APB group (APB_{high} (red) and APB_{low} (blue)). APB, alternate promoter use burden; TIL, tumour-infiltrating lymphocyte.

in the cohort had metastatic gastric cancer and had received at least one prior line of systemic therapy before entering an ICI clinical trial. Of the 53 samples, 13 tumours were classified as APB_{high}; 27 were classified as APB_{int}; and 13 were classified as APB_{low} (figure 4A). APB_{high} tumours had a significantly poorer progression-free survival (PFS) compared with APB_{int} (median PFS 55 vs 87 days, HR 0.39, 95% CI 0.19 to 0.80, p=0.01) and APB_{low} tumours (median PFS 55 vs 121 days, HR 0.40, 95% CI 0.18 to 0.93, p=0.032) (figure 4B). TCGA subtyping and PD-L1 immunohistochemistry data were available for 44 (83%) and 40 (75%) samples, respectively (online supplemental methods, table S5). EBV and MSI subtype tumours had a significantly higher PFS compared with CIN or GS tumours (median PFS not reached vs 80 days, HR 0.088, 95% CI 0.02 to 0.38, p=0.0011). PD-L1 combined positive score (CPS) ≥10 samples also had improved survival compared with CPS <10 (median PFS 254 vs 80 days, HR 0.33, 95% CI 0.13 to 0.87, p=0.025). These data are consistent with previous findings.[26 27] Of particular clinical interest is the identification of predictive biomarkers for immunotherapy in the PD-L1 CPS <10 and CIN/GS subgroups. We first studied APB in the PD-L1 CPS <10 subgroup (n=31) and found APB_{low} and APB_{int} tumours to have a significantly higher PFS compared with APB_{high} (median PFS 119 vs 84 vs 48 days, HR 0.22, 95% CI 0.08 to 0.62, p=0.0042) (online supplemental figure S4A). When the PD-L1 CPS <10 tumours were restricted to only the CIN/GS subtype (n=28), the results were similar (median PFS 109 (APB_{low}) vs 83 (APB_{int}) vs 48 days (APB_{high}), HR 0.27, 95% CI 0.097 to 0.74, p=0.012) (online supplemental figure S4B).

To assess the specificity of APB in predicting responses to ICIs, we next studied the role of APB in predicting sensitivity to other types of systemic therapy. We analysed a separate cohort of 60 metastatic STADs treated with chemotherapy (first-line 5-fluorouracil and platinum-based chemotherapy, online supplemental table S1). There was no difference in PFS between the three APB groups (median PFS 158 (APB_{high}) vs 129 (APB_{int}) vs 154 days (APB_{low}), p=0.9) (online supplemental figure S4C). To extend this to another systemic therapy regimen, we then tested an independent cohort of patients with gastric cancer treated

Gut: first published as 10.1136/gutjnl-2021-324420 on 25 August 2021. Downloaded from http://gut.bmj.com/ on April 17, 2024 by guest. Protected by copyright.

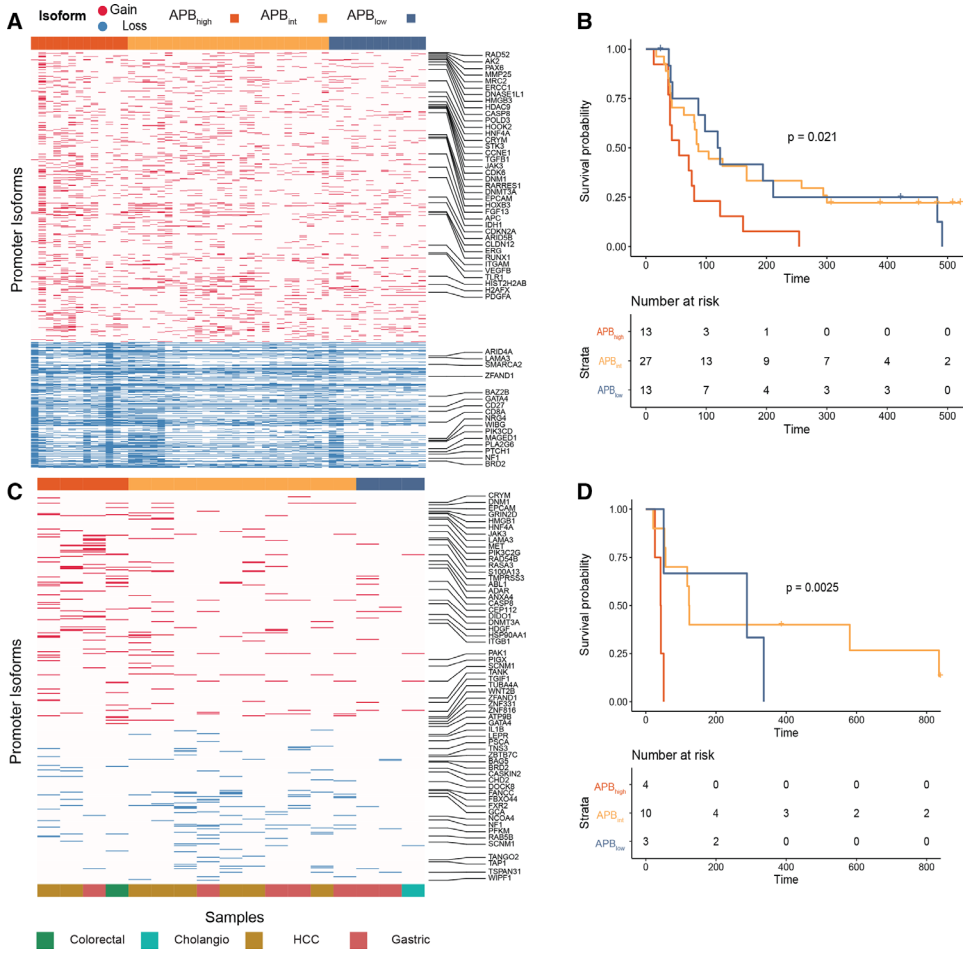

Figure 4 Resistance of APB_{high} tumours to immune checkpoint inhibition. (A) Heatmap of alternate promoter use of gastric cancer ICI-treated samples. Fifty-three gastric cancer ICI-treated samples (nivolumab, pembrolizumab and atezolizumab) were used for this analysis. Gain alternative promoter (marked red in the heatmap) and loss alternative promoter (marked blue in the heatmap) use (in columns) per sample (in rows). (B) Gastric cancer ICI PFS by APB group (n=53). Kaplan-Meier curve of PFS comparing APB_{high} (red) versus APB_{int} (yellow) versus APB_{low} (blue). P value is according to two-sided log-rank test. (C) Heatmap of alternate promoter use measured by NanoString of ICI-treated non-squamous samples. In total, archival tissue of 17 non-squamous ICI-treated samples were used for NanoString analysis to calculate the APB. Gain alternative promoter (marked red in the heatmap) and loss alternative promoter (marked blue in the heatmap) use (in columns) per sample (in rows). (D) Survival of NanoString cohort of ICI-treated non-squamous samples (n=17). Kaplan-Meier curve of PFS comparing APB_{high} (red) versus APB_{int} (yellow) versus APB_{low} (blue). P value is according to two-sided log-rank test. APB, alternate promoter use burden; ICI, immune checkpoint inhibitor; PFS, progression-free survival.

with a combination of chemotherapy and targeted therapy (paclitaxel and ramucirumab, n=47). We observed a similar lack of difference in PFS between the groups (median PFS 104 (APB_{high}) vs 128 (APB_{int}) vs 126 days (APB_{low}), p=0.8) (online supplemental figure S4D). These findings suggest that, within the limitations of the therapies tested, that the predictive nature of APB may be specific to ICI treatment.

For a large majority of clinical cohorts including those from clinical trials, only archival formalin fixed paraffin embedded (FFPE) tissue is available, which poses technical challenges, with respect to RNA extraction and characterisation using RNA-Seq.[28] The NanoString platform has been validated to generate predictive gene-expression signatures from FFPE tissue that has been used in clinical practice.[29] To explore additional cohorts, we thus designed a custom-made NanoString panel to infer APB in FFPE tissue, under the technical probe limitation of NanoString (800 probes). From 4519 promoters used to calculate the APB algorithm in RNA-Seq data, we identified the top-ranked promoters from the TCGA STAD analysis and designed alternate promoter probes for a NanoString panel. NanoString probes were designed to predominantly bind to the unique first exon junctions, allowing for identification and differentiation of alternate promoter transcripts. This approach is conceptually similar to the *proActiv* algorithm in identifying gain and loss promoter transcripts[13] (online supplemental methods). We tested a heterogenous cohort of 35 ICI-treated GI tumours using this custom-designed NanoString panel. The cohort included tumours of squamous (anal and oesophageal) (n=18) and non-squamous (colorectal, gastric, cholangiocarcinoma (CHOL) and hepatocellular carcinoma (HCC)) (n=17) histology. Patients were treated with a range of ICIs including nivolumab, avelumab and durvalumab (monoclonal antibodies against PD-1/PD-L1). In the non-squamous cohort, APB_{high} tumours had inferior survival compared with APB_{low} tumours (median PFS 43 vs 288 days, HR 0.10, 95% CI 0.01 to 0.78, p=0.028) (figure 4C,D). Similar results could not be replicated in the squamous cancer cohort (median PFS APB_{high} 241 days vs APB_{int} 142 days vs APB_{low} 216 days, p=0.99) (see the Discussion section). To further improve on APB measured through NanoString (online supplemental methods), we performed an analysis on archival FFPE tissue

Gut: first published as 10.1136/gutjnl-2021-324420 on 25 August 2021. Downloaded from http://gut.bmj.com/ on April 17, 2024 by guest. Protected by copyright.

of 53 patients with gastric cancer treated with anti-PD-1 axis therapy (online supplemental table S1). APB was inferred using a similar formula and identified 13 APB_{high}, 20 APB_{int} and 20 APB_{low} samples. PFS of APB_{high} patients was significantly lower compared with APB_{int} and APB_{low} patients (48 vs 64 vs 175 days, HR (APB_{high} vs APB_{low}) 0.25, 95% CI 0.11 to 0.57, p=0.001) (online supplemental figure S4E).

Having shown that APB could be potentially applied to other GI tumour types, we also studied RNA-Seq data of 66 HCC samples, of which 26 were treated with nivolumab and 40 were treated with pembrolizumab. Seventeen tumours were classified as APB_{high}; 32 were classified as APB_{int}; and 17 were classified as APB_{low}. APB_{low} tumours had a significantly better PFS compared with APB_{int}/APB_{high} tumours (median PFS 242 vs 90 vs 94 days, HR 0.51, 95% CI 0.27 to 0.99, p=0.046) (online supplemental figure S4F). Taken collectively, these findings suggest that our initial conclusions on gastric cancer could be expanded to GI tumours with high alternate promoter use, exhibiting a higher probability of primary resistance to immune checkpoint inhibition and suggesting a role for using APB as a predictive biomarker for immunotherapy.

High APB is associated with an immunologically quiet phenotype across multiple tumour types

Finally, to explore associations between APB and the immune tumour microenvironment in a wide set of tumour types, we quantified APB for 10 165 samples across 26 tumour types from the TCGA PanCanAtlas RNA-Seq database. Tumours were categorised into APB_{high}, APB_{low} and APB_{int} subgroups based on tumour type-specific quartiles (online supplemental figure S5A). Similar to STADs, the majority of tumour types exhibited a significant correlation between the APB groups and *CD8A*, *GZMA* and *PRF1* expression. Specifically, of the 26 tumour types analysed, 16 (62%) had significant correlations with all three markers (figure 5A and online supplemental table S6). Only three tumour types had no correlation between APB and *CD8A*, *GZMA* or *PRF1* (adrenocortical carcinoma (ACC), CHOL and uveal melanoma (UVM)). Notably, these latter three cohorts (ACC, CHOL and UVM) are all of relatively small sample sizes (n<100, median tumour-type dataset size=414). These results suggest that APB is associated with features of the immune microenvironment across multiple tumour types.

To investigate additional immunological phenotypes associated with high APB, genome-wide expression differences between APB_{high} and APB_{low} tumours were identified. From a total of ~20 000 genes compared, we selected the Immport subset—a database of ~4000 genes with immune-related functions and interactions.[30] A larger number of Immport immune genes exhibited high expression in APB_{low} tumours relative to APB_{high} tumours for several tumour-types (threshold: fold change >1.5, adjusted p value<0.01). For example, in breast cancer, Immport gene sets were significantly overexpressed in APB_{low} tumours (APB_{low}: 731 genes vs APB_{high}: 339, p≤0.0001). Differential expressions of selected immune checkpoint genes (*PD-1*, *PD-L1*, *PD-L2*, *CTLA4*, *LAG3*, *TIM3*, *ICOS*, *BTLA* and *TIGIT*) were also studied between the APB groups. Similar to STAD, almost all immune checkpoints were overexpressed in APB_{low} tumours for a majority of tumour types (figure 5B). We also leveraged a pan-cancer TCGA study classifying tumours by immune signatures.[22] APB_{low} tumours were found to have higher lymphocyte infiltration signature scores and interferon-γ response signatures (p<0.0001) (online supplemental figure S5B,C).

MSI status was available for 7919 samples, of which 176 tumours (2%) were found to be MSI-high. The prevalence of MSI-high in the APB groups was 3.3% APB_{low}, 2.5% APB_{int} and 1.5% APB_{high} (Fisher's exact p=0.0016). Thus, similar to findings in STAD, there appears to be a trend for MSI-high tumours to be classified as APB_{low} (33% of all MSI-high tumours were APB_{low} compared with 15% being APB_{high}), although it is worth noting that MSI-high tumours are found in all three APB groups. There was no correlation between APB and TMB (median APB_{low} 1.8 vs APB_{int} 1.8 vs APB_{high} 1.8 muts/Mb, p=0.64) (online supplemental figure S5D). Within MSI-H tumours, there was no difference in TMB between APB_{high} and APB_{low} (p=0.13). Taken collectively, these results, based on gene expression analyses at the global, immune checkpoint and immune signature levels, suggest that APB_{high} tumours are consistently associated with an immunologically 'cold' tumour phenotype.

DISCUSSION

In this study, we sought to explore the role of alternate promoter use in cancer immunity and therapy response. Our results extend previous findings applying H3K4me3 histone profiling on primary STADs to infer promoter activity where tumour-associated promoter isoforms recurrently lost in STADs exhibited a significant enrichment in high-affinity major histocompatibility complex class I binding peptides.[9] We proposed that this may reflect a novel tumour immune-editing mechanism where promoter alterations are used to evade the host immune system, thereby facilitating nascent tumour development.

Usage of alternate promoters at cancer-related genes such as *NOTCH* has been described to play a role in T-cell development and carcinogenesis, while in EBV-associated Natural Killer T-cell lymphoma, downregulation of immunogenic viral nuclear antigens through alternate promoter use has been proposed as a mechanism of immune escape.[31 32] In our study, we found pervasive genome-wide usage of alternate promoters by tumours which was associated with evidence of immune-editing and evasion. It is worth noting that these associations were observed in multiple tumour types, despite using a set of promoters originally derived from STADs. It is possible that alternate promoter usage may be less related to specific tissue of origin and reflects a conserved pan-cancer response to host immunity. Correlation between alternate promoter use, TMB and MSI indicates that APB interacts with the tumour immune microenvironment through an independent mechanistic pathway, distinct from acquisition of DNA somatic mutations (represented by TMB and MSI status). Through correlative analysis of APB with tumour content and clonal heterogeneity, we also demonstrated that promoter alterations are driven through polyclonal mechanisms.

To assess the tumour microenvironment from bulk RNA-Seq data, we used expression of specific genes such as *CD8A*, *GZMA* and *PRF1* as surrogates. Using single-cell RNA-Seq, which allows for identification and characterisation of different cellular subtypes within a heterogenous tumour microenvironment,[33] we validated the use of these surrogate markers by confirming that the expressions of these genes are largely restricted only to immune cells of interest. Our scRNA-Seq also describes the expression of various immune checkpoints by cell type in STAD. These findings, along with others describing the immune contexture in STAD, form an important resource for the development of cellular therapies and novel checkpoint inhibitor combinations and strategies.[34] Our scRNA-Seq dataset included samples from various TCGA subtypes including CIN, GS and MSI. A limitation of our study is that we could not include EBV gastric

Gut: first published as 10.1136/gutjnl-2021-324420 on 25 August 2021. Downloaded from http://gut.bmj.com/ on April 17, 2024 by guest. Protected by copyright.

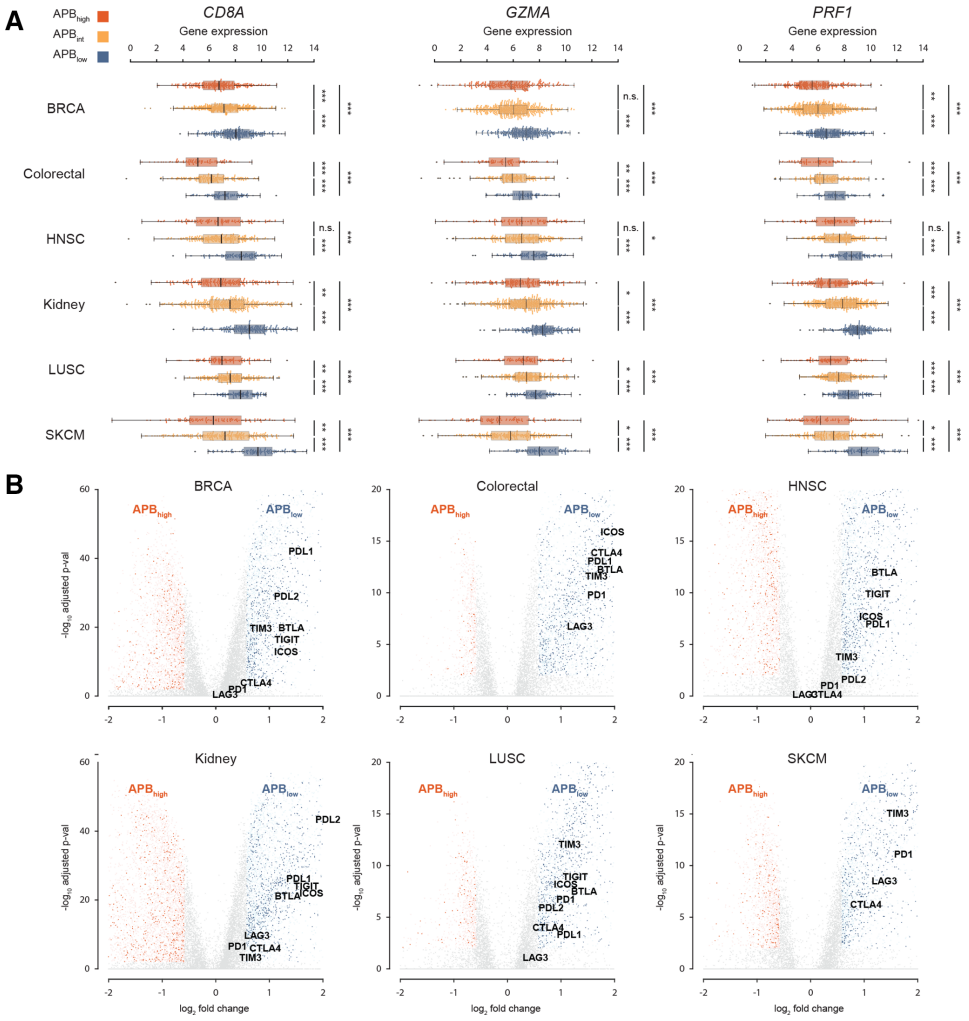

Figure 5 Pan-cancer APB association with immune correlates. (A) Association of APB groups in breast (BRCA), colorectal, head and neck (HNSC), kidney, squamous lung (LUSC) and melanoma (SKCM) with markers of T-cell cytolytic activity (*CD8A*, *GZMA* and *PRF1*). The APB_{high} group is denoted in red, APB_{int} in yellow and APB_{low} in blue. The APB_{high} group shows lower expression of these three genes compared with APB_{int}, which in turn shows a lower expression to the APB_{low} group (Wilcoxon test; ***p<0.001, **p<0.01, *p<0.05; n.s.). (B) Volcano plot of ~20 000 genes in the PanCanAtlas correlated with APB_{high} and APB_{low} for six tumour types (BRCA, colorectal, HNSC, kidney, LUSC and SKCM). The x-axis is the log_2FC of gene expression (RSEM) between APB_{high} and APB_{low}. The y-axis is the $-log_{10}$ adjusted p value results (Bonferroni correction). Genes that are at least >1.5× fold change and adjusted p<0.01 are coloured, while the rest are grey. Immune genes that are overexpressed APB_{high} are dark red, while non-immune genes are pale red. Similarly, APB_{low} overexpressed immune genes are dark blue, while non-immune genes are pale blue. Nine selected immune checkpoints (*PD1*, *PD-L1*, *PD-L2*, *LAG3*, *CTLA4*, *TIM3*, *ICOS*, *TIGIT* and *BTLA*) are labelled. As a general trend, immune checkpoints appear to be overexpressed in APB_{low} tumours. APB, alternate promoter use burden; HNSC, head and neck squamous cell; log_2FC, log_2 fold change; LUSC, lung squamous; n.s., not significant; SKCM, melanoma.

cancer, which is associated with high levels of T-cell infiltration and PD-L1 expression.[35] EBV tumours tend to be more indolent, detected at earlier stages, and constitute the smallest subtype of gastric cancer in the TCGA (9%), with an even lower incidence in Asian cohorts (8%).[36] Another interesting finding in our study was the higher levels of mast cells detected in the APB_{high} STAD TCGA cohort samples. Mast cells are tissue-resident innate immune cells that have been associated with both activation and downregulation of adaptive and innate immune responses,[37] and whose activity can be mediated by epigenetic regulators.[38] Mast cells ameliorate effector T-cell function by inhibiting regulatory T cells through the OX40 axis.[39] Higher mast cells in APB_{high} tumours may reflect a compensatory upregulation of innate immunity due to the lower levels of T cells (adaptive immunity).[40]

For this study, we established an in vivo model to study the dynamic temporal interactions between alternate promoter use and the human immune system. While generating the model, we considered several factors—first, the model required a functional immune system, thereby prohibiting the use of conventional immunodeficient mice. Second, as the model had to allow testing of tumours with diverse molecular phenotypes; traditional syngeneic murine models where tumours are derived from the same genetic background as the host mouse were ruled out. The humanised mouse model bridges a significant gap from traditional human patient-derived xenograft models which are grown in immunodeficient mice, or in vitro cell-line/T-cell co-culture models for testing of tumour-immune interactions.[41] Humanised-mouse models have been used to study HCC, lung cancer, sarcoma and breast cancer.[41 42] Our study is the first to

Gut: first published as 10.1136/gutjnl-2021-324420 on 25 August 2021. Downloaded from http://gut.bmj.com/ on April 17, 2024 by guest. Protected by copyright.

analyse STADs using humanised mice and employ experimental designs mirroring preceding studies, comparing tumour growth kinetics between humanised-mice and immune deficient mice. APB_{low} tumours appeared to grow later and slower in humanised mice compared with immune-deficient mice and to APB_{high} tumours. Similar findings were seen in triple negative breast cancers, where tumours grew faster in immune-deficient mice compared with humanised mice.[42] Increased presence of cytotoxic T cells within the tumours limiting growth in humanised mice was demonstrated in an HCC study, and treatment with pembrolizumab demonstrated a further increase of TILs.[41] Notably, harvesting and analysing the tumours at the end of our experiment to evaluate the tumour immune microenvironment demonstrated the lack of TILs in APB_{high} tumours, a finding consistent with the other experiments in our study. The humanised-mouse model developed in this study is an ideal platform to test therapeutic strategies such as these, which target the tumour−immune system interface. However, one of the limitations is the treatment of the model with immunotherapy and epigenetic agents will require rigorous optimisation and controlling as the platform has not been used in gastric cancer models previously. Other limitations of the mouse-model experiment include the subcutaneous flank injection of the tumours. Intragastric transplantation of tumours has been described in immune-deficient patient-derived organoid models and could potentially be incorporated in future humanised-mouse experiments with gastric cancer.[43 44]

Prognostic biomarkers guide on patient outcomes or survival regardless of therapy, while predictive biomarkers provide information on the effectiveness of a specified therapy.[45] Currently, the most developed predictive biomarkers for ICI are PD-L1 expression measured by immunohistochemistry, MSI and TMB.[46 47] These biomarkers are positive predictive biomarkers that identify tumours that are likely to respond to ICI. However, controversies surrounding these biomarkers have been raised and ICI responses in biomarker-negative populations have been observed.[48] These observations highlight the complementary role of negative predictive biomarkers for ICIs that identify tumours resistant to therapy, similar to *RAS* mutations in colorectal cancer that predict resistance to anti-EGFR therapies.[49] By analysing the predictive value of APB in chemotherapy and targeted therapy cohorts as well,[50 51] we confirmed that within the limitations of the therapies tested, the predictive nature of APB may be specific to ICI treatment. Our findings may guide selection of patients with gastric cancer for immunotherapy treatment by categorising patients into three groups: first, the 'likely responders', which consist of MSI-H, EBV and PD-L1 CPS ≥10 subgroups. Second, the 'unlikely responders', consisting of APB_{high} patients, with the remaining patients falling to the third category of 'possible responders'. The remaining third group of patients tends to demonstrate moderate benefit from immunotherapy but with earlier resistance and modest PFS.

Sensitivity to immune checkpoint inhibition is driven through various factors including neoantigen formation, tumour mutational burden and PD-L1 expression.[47] Our cohort of GI squamous cell cancers consisted of oesophageal and anal carcinoma, while our APB algorithm was derived from adenocarcinoma samples of gastric cancer origin. The TCGA comparison of squamous and adenocarcinoma histological subtypes of the oesophagus has also identified significant genomic and epigenetic differences.[52] Squamous oesophageal cancer has also been shown to have a significantly higher proportion of responses to immune checkpoint inhibition compared with oesophageal adenocarcinoma, driven by higher PD-L1 expression.[52 53] A similar high response rate of squamous anal carcinoma to pembrolizumab has also been demonstrated.[54] These results were reflected in our cohort as well, with 72% of patients having disease control (stable disease or partial response) as best response to ICI in the squamous cohort, compared with 41% in the adenocarcinoma cohort. Thus, as our APB algorithm appears to best function as a negative predictive biomarker, identifying poor responders to ICI, the high sensitivity of squamous cancers to ICI and small numbers may be reasons for the NanoString panel failing to differentiate responders and non-responders in the squamous GI cancer cohort. The identification of a subgroup of tumours exhibiting primary resistance to immunotherapy that are associated with alternate promoters raises intriguing possibilities for biomarker-selected combination therapeutic strategies. Drugs targeting epigenetic pathways such as DNA methyltransferase and histone deacetylase have been shown to abrogate immune evasion through targeting mechanisms such as antigen processing and presentation, expression of chemokines and immune checkpoints, and host immune priming.[55] Several trials are currently ongoing, looking at the role of combining epigenetic agents with ICI, aiming to convert immunologically 'cold' to 'hot' tumours that may be more sensitive to immunotherapy.[55–57]

In conclusion, our study describes alternate promoter usage as a conserved pan-cancer marker that is associated with an immune-depleted tumour microenvironment, and quantification of APB may serve as a novel negative predictive biomarker of immune checkpoint inhibition.

Author affiliations
[1]Department of Haematology-Oncology, National University Cancer Institute, Singapore, National University Hospital, Singapore
[2]Yong Loo Lin School of Medicine, National University of Singapore, Singapore
[3]Cancer and Stem Cell Biology Program, Duke-NUS Medical School, Singapore
[4]The N.1 Institute for Health, National University of Singapore, Singapore
[5]Singapore Gastric Cancer Consortium, Singapore
[6]Genome Institute of Singapore, Agency for Science, Technology and Research, Singapore
[7]Institute of Molecular and Cell Biology, Agency for Science, Technology and Research, Singapore
[8]Diagnostic Development Hub (DxD), Agency for Science, Technology and Research, Singapore
[9]Division of Medical Oncology, National Cancer Centre, Singapore
[10]Curie Oncology, Singapore
[11]Department of Development Sciences, Genentech, San Francisco, California, USA
[12]Medical Oncology Department, Fondazione IRCCS Istituto Nazionale dei Tumori, Milan, Italy
[13]Division of Hematology-Oncology, Department of Medicine, Samsung Medical Center, Sungkyunkwan University School of Medicine, Seoul, South Korea
[14]Cancer Science Institute of Singapore, National University of Singapore, Singapore
[15]Statistical Programming and Analytics, Roche Canada, Mississauga, Ontario, Canada
[16]University Health Network, Toronto, Ontario, Canada
[17]Sci-illustrate, Munich, Germany
[18]InSilico Genomics, Phoenix, Arizona, USA
[19]Laboratory of Cancer Epigenome, Department of Medical Sciences, National Cancer Centre, Singapore
[20]Division of Medical Oncology, Department of Internal Medicine, Yonsei Cancer Center, Yonsei University College of Medicine, Seoul, South Korea
[21]Songdang Institute for Cancer Research, Yonsei University College of Medicine, Seoul, South Korea
[22]Department of Clinical Oncology, Aichi Cancer Center Hospital, Nagoya, Japan
[23]Department of Surgery, National University Hospital, Singapore
[24]Department of Surgery, Yong Loo Lin School of Medicine, National University of Singapore, Singapore
[25]Department of Microbiology and Immunology, Yong Loo Lin School of Medicine, National University of Singapore, Singapore
[26]SingHealth/Duke-NUS Institute of Precision Medicine, National Heart Centre, Singapore
[27]Department of Physiology, Yong Loo Lin School of Medicine, National University of Singapore, Singapore

Gut: first published as 10.1136/gutjnl-2021-324420 on 25 August 2021. Downloaded from http://gut.bmj.com/ on April 17, 2024 by guest. Protected by copyright.

Acknowledgements We thank the patients and their families for participating in our trials and magnanimously providing consent for the use of tissue to further the science.

Contributors Conceptualisation: RS, AQ, JG and PT; data curation: RS, KKH, DD, VK, KR, ZH, XO, ZFBAI, MX, AL-KT, DWMT, WZ, SPC, JQL, MDT, LM, EC, MF, MN, FP, JL, JY, CCYN, SYR, JS, KM, YN, WPY, QC and JG; formal analysis: RS, KKH, AQ, VK, ADJ, MDS, YAG, AJS, JG and PT; funding acquisition: JG and PT; methodology: RS, VK, MDS, QC, DD, AQ, JG and PT; project administration: RS and PT; resources and supervision: QC, JG and PT; visualisation: RS, AQ, KKH, RP and AF; writing of the original draft: RS; writing (review and editing): ZH, QC, JG and PT; approval of final version of manuscript: all authors.

Funding RS is supported by a National Medical Research Council (NMRC) Fellowship (NMRC/Fellowship/0059/2018 and MOH-000627), Singapore. FP is supported by a research grant from Associazione Italiana per la Ricerca sul Cancro (AIRC IG 2019 Id.23624). PT is supported by Duke-NUS Medical School and the Biomedical Research Council, Agency for Science, Technology and Research. Humanised mouse work was supported by National Research Foundation Singapore Fellowship (NRF-NRFF2017-03) to QC. This work was also supported by National Medical Research Council grants OF-LCG18May-0023, NR13NMR111OM, and NMRC/STaR/0026/2015.

Competing interests The subject matter in this manuscript was submitted as a technology disclosure to the institutional Technology Transfer Office for potential intellectual property protection. PT had stock and other ownership interests in HealthSeq, research funding from Kyowa Hakko Kirin and Thermo Fisher Scientific, and patents/other intellectual property through the Agency for Science and Technology Research, Singapore (all outside the submitted work). RS received honoraria from Bristol-Myers Squibb, Lilly, Roche, Taiho, Astra Zeneca, DKSH and MSD; had advisory activity with Bristol-Myers Squibb, Eisai, Merck, Bayer, Taiho, Novartis, MSD and AstraZeneca; received research funding from Paxman Coolers and MSD; received travel grants from AstraZeneca, Roche, Eisai and Taiho Pharmaceutical (all outside the submitted work). FP received honoraria for speakers' bureau/advisory activity from Amgen, Merck-Serono, Roche, Lilly, Sanofi, Bayer and Servier, and received research funding from BMS (all outside the submitted work).

Patient consent for publication Not required.

Ethics approval The study was approved by the local ethics board (DSRB reference number 2005/00440).

Provenance and peer review Not commissioned; externally peer reviewed.

Data availability statement Data used in this manuscript includes previously published studies with genomic data files from public repositories: European Nucleotide Archive: PRJEB25780 and PRJEB34724 The Cancer Genome Atlas Research Network: dbGaP: phs000178.v10.p8

Supplemental material This content has been supplied by the author(s). It has not been vetted by BMJ Publishing Group Limited (BMJ) and may not have been peer-reviewed. Any opinions or recommendations discussed are solely those of the author(s) and are not endorsed by BMJ. BMJ disclaims all liability and responsibility arising from any reliance placed on the content. Where the content includes any translated material, BMJ does not warrant the accuracy and reliability of the translations (including but not limited to local regulations, clinical guidelines, terminology, drug names and drug dosages), and is not responsible for any error and/or omissions arising from translation and adaptation or otherwise.

Open access This is an open access article distributed in accordance with the Creative Commons Attribution Non Commercial (CC BY-NC 4.0) license, which permits others to distribute, remix, adapt, build upon this work non-commercially, and license their derivative works on different terms, provided the original work is properly cited, appropriate credit is given, any changes made indicated, and the use is non-commercial. See: http://creativecommons.org/licenses/by-nc/4.0/.

ORCID iDs
Kie-Kyon Huang http://orcid.org/0000-0003-4104-8951
Aditi Qamra http://orcid.org/0000-0003-2977-0087
Qingfeng Chen http://orcid.org/0000-0001-6437-1271
Patrick Tan http://orcid.org/0000-0002-0179-8048

REFERENCES

1 Hanahan D, Weinberg RA. Hallmarks of cancer: the next generation. *Cell* 2011;144:646–74.
2 Vinay DS, Ryan EP, Pawelec G, *et al*. Immune evasion in cancer: mechanistic basis and therapeutic strategies. *Semin Cancer Biol* 2015;35:S185–98.
3 Schreiber RD, Old LJ, Smyth MJ. Cancer Immunoediting: Integrating Immunity's Roles in Cancer Suppression and Promotion. *Science* 2011;331:1565–70.
4 Baylin SB. Dna methylation and gene silencing in cancer. *Nat Clin Pract Oncol* 2005;2:S4–11.
5 Chiappinelli KB, Strissel PL, Desrichard A, *et al*. Inhibiting DNA methylation causes an interferon response in cancer via dsRNA including endogenous retroviruses. *Cell* 2015;162:974–86.
6 Jung H, Kim HS, Kim JY, *et al*. Dna methylation loss promotes immune evasion of tumours with high mutation and copy number load. *Nat Commun* 2019;10:4278.
7 Philip M, Fairchild L, Sun L, *et al*. Chromatin states define tumour-specific T cell dysfunction and reprogramming. *Nature* 2017;545:452–6.
8 Bennett RL, Licht JD. Targeting epigenetics in cancer. *Annu Rev Pharmacol Toxicol* 2018;58:187–207.
9 Qamra A, Xing M, Padmanabhan N, *et al*. Epigenomic promoter alterations amplify gene isoform and immunogenic diversity in gastric adenocarcinoma. *Cancer Discov* 2017;7:630–51.
10 Sundar R, Huang KK, Qamra A, *et al*. Epigenomic promoter alterations predict for benefit from immune checkpoint inhibition in metastatic gastric cancer. *Annals of Oncology* 2019;30:424–30.
11 Davuluri RV, Suzuki Y, Sugano S, *et al*. The functional consequences of alternative promoter use in mammalian genomes. *Trends Genet* 2008;24:167–77.
12 Bieberstein NI, Carrillo Oesterreich F, Straube K, *et al*. First exon length controls active chromatin signatures and transcription. *Cell Rep* 2012;2:62–8.
13 Demircioğlu D, Cukuroglu E, Kindermans M, *et al*. A pan-cancer transcriptome analysis reveals pervasive regulation through alternative promoters. *Cell* 2019;178:1465–77.
14 Butler A, Hoffman P, Smibert P, *et al*. Integrating single-cell transcriptomic data across different conditions, technologies, and species. *Nat Biotechnol* 2018;36:411–20.
15 Stuart T, Butler A, Hoffman P, *et al*. Comprehensive integration of single-cell data. *Cell* 2019;177:1888–902.
16 Zhang P, Yang M, Zhang Y, *et al*. Dissecting the single-cell transcriptome network underlying gastric premalignant lesions and early gastric cancer. *Cell Rep* 2019;27:1934–47.
17 Deng M, Brägelmann J, Kryukov I, *et al*. FirebrowseR: an R client to the Broad Institute's Firehose Pipeline. *Database* 2017;2017:baw160.
18 Furey TS. Chip-Seq and beyond: new and improved methodologies to detect and characterize protein-DNA interactions. *Nat Rev Genet* 2012;13:840–52.
19 Valcárcel LV, Amundarain A, Kulis M, *et al*. Gene expression derived from alternative promoters improves prognostic stratification in multiple myeloma. *Leukemia* 2021. doi:10.1038/s41375-021-01263-9. [Epub ahead of print: 10 May 2021].
20 Rooney MS, Shukla SA, Wu CJ, *et al*. Molecular and genetic properties of tumors associated with local immune cytolytic activity. *Cell* 2015;160:48–61.
21 Ghoshdastider U, Rohatgi N, Mojtabavi Naeini M, *et al*. Pan-Cancer analysis of ligand-receptor cross-talk in the tumor microenvironment. *Cancer Res* 2021;81:1802–12.
22 Thorsson V, Gibbs DL, Brown SD, *et al*. The immune landscape of cancer. *Immunity* 2018;48:812–30.
23 Ku J-L, Kim K-H, Choi J-S, *et al*. Establishment and characterization of six human gastric carcinoma cell lines, including one naturally infected with Epstein-Barr virus. *Cell Oncol* 2012;35:127–36.
24 Ku J-L, Park J-G. Biology of SNU cell lines. *Cancer Res Treat* 2005;37:1–19.
25 Kneissl J, Hartmann A, Pfarr N, *et al*. Influence of the her receptor ligand system on sensitivity to cetuximab and trastuzumab in gastric cancer cell lines. *J Cancer Res Clin Oncol* 2017;143:573–600.
26 Kim ST, Cristescu R, Bass AJ, *et al*. Comprehensive molecular characterization of clinical responses to PD-1 inhibition in metastatic gastric cancer. *Nat Med* 2018;24:1449–58.
27 Shitara K, Özgüroğlu M, Bang Y-J, *et al*. Pembrolizumab versus paclitaxel for previously treated, advanced gastric or gastro-oesophageal junction cancer (KEYNOTE-061): a randomised, open-label, controlled, phase 3 trial. *Lancet* 2018;392:123–33.
28 Hong M, Tao S, Zhang L, *et al*. Rna sequencing: new technologies and applications in cancer research. *J Hematol Oncol* 2020;13:166.
29 Wallden B, Storhoff J, Nielsen T, *et al*. Development and verification of the PAM50-based Prosigna breast cancer gene signature assay. *BMC Med Genomics* 2015;8:54.
30 Bhattacharya S, Dunn P, Thomas CG, *et al*. ImmPort, toward repurposing of open access immunological assay data for translational and clinical research. *Sci Data* 2018;5:180015.
31 Gómez-del Arco P, Kashiwagi M, Jackson AF, *et al*. Alternative promoter usage at the Notch1 locus supports ligand-independent signaling in T cell development and leukemogenesis. *Immunity* 2010;33:685–98.
32 Shen L, Chiang AKS, Liu WP, *et al*. Expression of HLA class I, ?2-microglobulin, TAP1 and IL-10 in Epstein-Barr virus-associated nasal NK/T-cell lymphoma: Implications for tumor immune escape mechanism. *Int J Cancer* 2001;92:692–6.
33 Hwang B, Lee JH, Bang D. Single-Cell RNA sequencing technologies and bioinformatics pipelines. *Exp Mol Med* 2018;50:1–14.
34 Fu K, Hui B, Wang Q, *et al*. Single-Cell RNA sequencing of immune cells in gastric cancer patients. *Aging* 2020;12:2747–63.
35 Sundar R, Qamra A, Tan ALK, *et al*. Transcriptional analysis of immune genes in Epstein-Barr virus-associated gastric cancer and association with clinical outcomes. *Gastric Cancer* 2018;21:1064–70.
36 Murphy G, Pfeiffer R, Camargo MC, *et al*. Meta-Analysis shows that prevalence of Epstein-Barr virus-positive gastric cancer differs based on sex and anatomic location. *Gastroenterology* 2009;137:824–33.

Gut: first published as 10.1136/gutjnl-2021-324420 on 25 August 2021. Downloaded from http://gut.bmj.com/ on April 17, 2024 by guest. Protected by copyright.

37 Rigoni A, Colombo MP, Pucillo C. The role of mast cells in Molding the tumor microenvironment. *Cancer Microenviron* 2015;8:167–76.
38 Monticelli S, Leoni C. Epigenetic and transcriptional control of mast cell responses. *F1000Res* 2017;6:2064.
39 Piconese S, Gri G, Tripodo C, *et al*. Mast cells counteract regulatory T-cell suppression through interleukin-6 and OX40/OX40L axis toward Th17-cell differentiation. *Blood* 2009;114:2639–48.
40 Slack E, Hapfelmeier S, Stecher B, *et al*. Innate and adaptive immunity cooperate flexibly to maintain host-microbiota mutualism. *Science* 2009;325:617–20.
41 Zhao Y, Shuen TWH, Toh TB, *et al*. Development of a new patient-derived xenograft humanised mouse model to study human-specific tumour microenvironment and immunotherapy. *Gut* 2018;67:1845–54.
42 Wang M, Yao L-C, Cheng M, *et al*. Humanized mice in studying efficacy and mechanisms of PD-1-targeted cancer immunotherapy. *Faseb J* 2018;32:1537–49.
43 Busuttil RA, Liu DS, Di Costanzo N, *et al*. An orthotopic mouse model of gastric cancer invasion and metastasis. *Sci Rep* 2018;8:825.
44 Reddavid R, Corso S, Moya-Rull D, *et al*. Patient-Derived orthotopic xenograft models in gastric cancer: a systematic review. *Updates Surg* 2020;72:951–66.
45 Oldenhuis CNAM, Oosting SF, Gietema JA, *et al*. Prognostic versus predictive value of biomarkers in oncology. *Eur J Cancer* 2008;44:946–53.
46 Lim JS, Sundar R, Chénard-Poirier M, *et al*. Emerging biomarkers for PD-1 pathway cancer therapy. *Biomark Med* 2017;11:53–67.
47 Sundar R, Smyth EC, Peng S, *et al*. Predictive biomarkers of immune checkpoint inhibition in gastroesophageal cancers. *Front Oncol* 2020;10:763.
48 Havel JJ, Chowell D, Chan TA. The evolving landscape of biomarkers for checkpoint inhibitor immunotherapy. *Nat Rev Cancer* 2019;19:133–50.
49 Sundar R, Tan IBH, Chee CE. Negative predictive biomarkers in colorectal cancer: PRESSING ahead. *JCO* 2019;37:3066–8.
50 Yong WP, Rha SY, Tan IB-H, *et al*. Real-Time Tumor Gene Expression Profiling to Direct Gastric Cancer Chemotherapy: Proof-of-Concept "3G" Trial. *Clinical Cancer Research* 2018;24:5272–81.
51 Kim ST, Sa JK, Oh SY, *et al*. Comprehensive molecular characterization of gastric cancer patients from phase II second-line ramucirumab plus paclitaxel therapy trial. *Genome Med* 2021;13:11.
52 Cancer Genome Atlas Research Network, Analysis Working Group: Asan University, BC Cancer Agency, *et al*. Integrated genomic characterization of oesophageal carcinoma. *Nature* 2017;541:169–75.
53 Kojima T, Shah MA, Muro K, *et al*. Randomized phase III KEYNOTE-181 study of pembrolizumab versus chemotherapy in advanced esophageal cancer. *JCO* 2020;38:4138–48.
54 Ott PA, Piha-Paul SA, Munster P, *et al*. Safety and antitumor activity of the anti-PD-1 antibody pembrolizumab in patients with recurrent carcinoma of the anal canal. *Ann Oncol* 2017;28:1036–41.
55 Dunn J, Rao S. Epigenetics and immunotherapy: the current state of play. *Mol Immunol* 2017;87:227–39.
56 Chiappinelli KB, Zahnow CA, Ahuja N, *et al*. Combining epigenetic and immunotherapy to combat cancer. *Cancer Res* 2016;76:1683–9.
57 Meric-Bernstam F, Larkin J, Tabernero J, *et al*. Enhancing anti-tumour efficacy with immunotherapy combinations. *Lancet* 2021;397:1010–22.

Gut: first published as 10.1136/gutjnl-2021-324420 on 25 August 2021. Downloaded from http://gut.bmj.com/ on April 17, 2024 by guest. Protected by copyright.